

This is the preprint of the contribution published as:

Balda, M., Mackenzie, K., Kopinke, F.-D., Georgi, A. (2022):
Uniform and dispersible carbonaceous microspheres as quasi-liquid sorbent
Chemosphere **307** (4), art. 136079

The publisher's version is available at:

<http://dx.doi.org/10.1016/j.chemosphere.2022.136079>

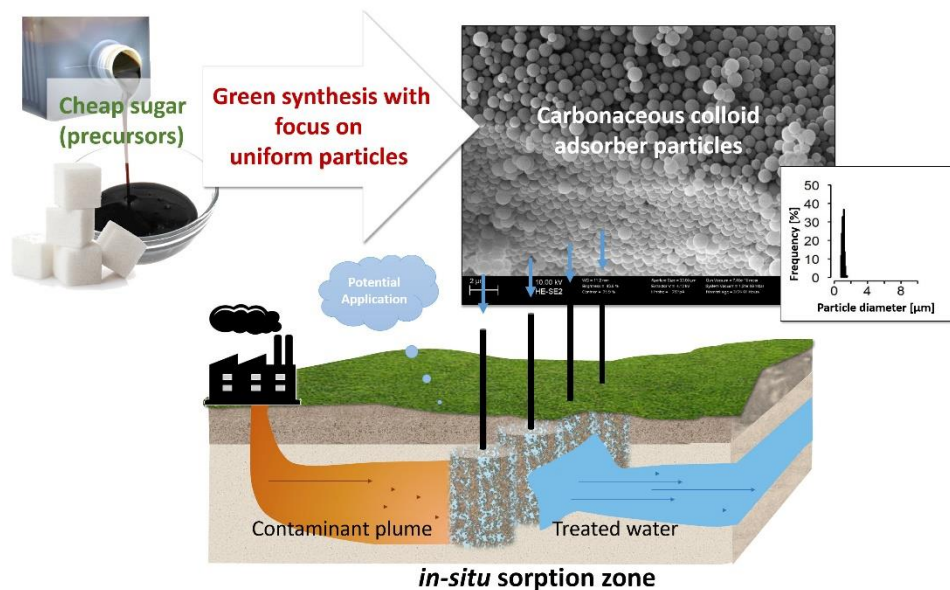
Uniform and Dispersible Carbonaceous Microspheres as Quasi-Liquid Sorbent

Maria Balda*, Katrin Mackenzie, Frank-Dieter Kopinke, Anett Georgi

Department of Environmental Engineering, Helmholtz Centre for Environmental Research –
UFZ, D-04318 Leipzig, Germany

Abstract

Functional
colloidal
carbon
materials find
various
applications,
including the
remediation of
contaminated



water and soil in so-called particle-based *in-situ* remediation processes. In this study, uniform and highly dispersible micro-sized carbonaceous spheres (CS) were generated by hydrothermal carbonization (HTC) of sucrose in the presence of carboxymethyl cellulose (CMC) as

* Corresponding author: maria.balda@ufz.de

environmentally friendly polyelectrolyte stabilizer. In order to ensure their optimal subsurface delivery and formation of a self-contained treatment zone, a narrow size distribution and low agglomeration tendency of the particles is desired. Therefore, the obtained CS were thoroughly characterized and optimized with respect to their colloidal properties which are a crucial factor for their application as quasi-liquid sorbent. The as-prepared uniform CS are readily dispersible into single particles in water, as confirmed by digital microscopy and form stable suspensions. Due to their perfectly spherical shape, particle sedimentation in aqueous suspensions is well predicted by Stokes' law. High sorption coefficients on the synthesized CS $K_{D,CS}$ were determined for phenanthrene (up to $\log(K_{D,CS} / [L\ kg^{-1}]) = 5$) and other hydrophobic groundwater contaminants. This confirms the application potential of the CS, which were prepared by an economic low-temperature process using sucrose as bio-based precursor, for generating *in-situ* sorption barriers for groundwater and soil remediation.

Keywords

Hydrothermal carbonization, uniform carbonaceous microspheres, dispersibility, CMC, sucrose, phenanthrene

1. Introduction

As water scarcity is an emerging problem worldwide, it becomes increasingly important to ensure the quality of existing water sources such as groundwater. Remediation of groundwater contamination due to past and ongoing industrial and other activities remains a demanding and costly task which requires continuous development towards more sustainable and cost-efficient technologies. For *ex-situ* treatment techniques, the contaminated groundwater has to be pumped up and either remediated on-site or transported to the treatment facility. This is why off-site techniques are mostly expensive and energy-intensive. A possible alternative are *in-situ* remediation techniques where adsorbents and/or reagents are directly injected into the

groundwater in order to bind or degrade pollutants directly at or close to the source of contamination (Zhang et al., 2019). These can either be dissolved chemicals such as permanganate, hydrogen peroxide or persulfate for *in-situ* chemical oxidation (ISCO) or particle-based adsorbents/reagents for the setting of permeable reactive barriers (PRBs) or retention zones within the aquifers.

The latter approach is termed particle-based *in-situ* remediation and makes use of colloidal materials which can be applied in quasi-liquid form to treat contaminations in the environment, forming stationary PRBs or zones in soils and aquifers by simple injection of adsorbent or reagent particles (Bardos et al., 2018). The most common nanoreagent is nanoscale zero-valent iron (NZVI) for contaminants which can be treated by reductive processes (Mackenzie and Georgi, 2019). At the same time, carbonaceous materials play an important role as adsorbents and carriers of reactants, whereby activated carbon in colloidal form (ACC) is the most prominent example which is applied at technical scale in remediation (Georgi et al., 2015; Carey et al., 2019; Sorengard et al., 2019; Intrapore, 2022). ACC is typically obtained from conventional activated carbon produced from coal, coconut shell or wood precursors in a top-down process by milling to a particle size of about 1 μm (Mackenzie et al., 2008; Georgi et al., 2015). ACC is applied in order to stop further spreading of pollutants with the groundwater flow, to reduce exposure and keep contaminants at place for further remediation measures such as stimulated biodegradation (Sorengard et al., 2019; Regensis, 2022).

Hydrothermal carbonization (HTC) is an alternative process for preparing carbon materials, whereby carbohydrates are dehydrated and polymerized into a char-like product in water at temperatures above 100 °C and self-generated pressures (Titirici and Antonietti, 2010). On the one hand, HTC can be used to convert waste biomass into carbonaceous materials, so-called hydrochars, which can subsequently be activated (Jain et al., 2016) or used as solid fuel (Nizamuddin et al., 2017). On the other hand, with the use of additives during the process, HTC also grants access to very specific carbon products such as hollow carbon spheres (White et al.,

2010; Yang et al., 2013), porous carbon spheres (Titirici et al., 2007; Kubo et al., 2013; Su et al., 2020), metal-carbon core-shell composites (Sun and Li, 2004; Yang et al., 2014; Liu et al., 2018a) or highly spherical carbonaceous particles (Sevilla and Fuertes, 2009a; Gong et al., 2014). Especially for synthesizing the latter, HTC is a rather elegant method because soluble carbohydrates such as mono-, di- and easily hydrolyzable polysaccharides naturally carbonize into a spherical shape during the hydrothermal process (Hu et al., 2010). Thus, HTC is able to produce colloidal particles directly in a low-temperature bottom-up approach whereas biochar formation from solid natural materials would require a high-temperature pyrolysis with subsequent milling steps. In addition, the HTC process results in a lignite-like carbon material which can be expected to have already exploitable sorption properties for hydrophobic contaminants. Adsorbent synthesis *via* HTC therefore deserves closer investigation as an alternative to the energy-intensive and CO₂-releasing high-temperature processes related to biochar and activated carbon production. The proposed underlying mechanism in HTC consists of three major steps: intramolecular dehydration of the saccharide into (hydroxymethyl)furfural (HMF) derivatives, polymerization of the former leading to soluble polymers, and particle formation *via* further intermolecular dehydration and crosslinking of said polymers (Li and Shahbazi, 2015). After reaching a critical supersaturation, nucleation occurs. Commonly, it was presumed that the formed nuclei grow according to the LaMer model (LaMer, 1952) by diffusion of the dissolved intermediates, e.g. HMF, to the carbon surface and reaction with the reactive oxygen functional groups (Sun and Li, 2004; Li and Shahbazi, 2015). However, it was recently shown by Jung *et al.* (2018) that the depletion of HMF is directly proportional to the formation of fresh hydrochar nuclei rather than particle growth (Jung et al., 2018). Only when the hydrochar nuclei formation rate decreases and HMF is depleted, do the particles grow increasingly. This suggests that the particles grow *via* agglomeration and inter-particle polymerization/carbonization (Jung et al., 2018).

When aiming for the efficient generation of uniform micrometer-sized carbonaceous spheres (CS) for particle-based *in-situ* remediation, two contrary aspects have to be considered: increasing carbohydrate concentration, reaction temperature and reaction time each lead to a greater mass yield of hydrochar (Sevilla and Fuertes, 2009a; Dinjus et al., 2011). However, simultaneously the CS become bigger, less uniform and less dispersible (Zheng et al., 2009; Jung et al., 2018).

The findings cited above on the inter-particle polymerization growth mechanism of HTC particles imply that efficient stabilization against agglomeration is a key factor for obtaining rather uniform particles instead of a wide size range of individual and aggregated particles.

There have been some studies of HTC with additives such as synthetic polymers/-electrolytes (Gong et al., 2014; Su et al., 2020) or even inorganic salts in large concentrations (Yang et al., 2016; Liang et al., 2019; Liu et al., 2019) in order to optimize the yield of uniform CS. However, the excessive use of salts or the addition of hazardous compounds compromise the sustainable character of the HTC process. Carboxymethyl cellulose (CMC) is known as a cheap, non-toxic and environmentally friendly stabilizing agent which is used in particle-based *in-situ* remediation to improve suspension stability and mobility of the particles during injections. It acts as particle dispersant by a combination of electrostatic and steric forces (Philippe and Schaumann, 2014; Mackenzie and Georgi, 2019). However, despite of its benign properties, CMC has not yet been tested as polyelectrolyte additive in HTC processes. Its application might even appear counterintuitive as it is subject to hydrolysis and/or carbonization under harsh HTC conditions (Falco et al., 2011).

In terms of potential application of HTC-derived carbonaceous particles, previous studies focused extensively on their adsorption behavior towards heavy metals (Zhao et al., 2013; Cai et al., 2016; Chowdhury et al., 2018; Liu et al., 2018b). However, there is little data on the sorption of organic compounds (Li et al., 2017). The actual colloidal properties of the particles such as the dispersibility of the synthesized CS and their suspension stability in aqueous media

are only mentioned in passing (Sun and Li, 2004; Yang et al., 2014) and have, to the best of our knowledge, not yet been studied in detail. The mentioned characteristics are linked to the surface charge of the particles as well as their size distribution and shape, and strongly determine their injectability and mobility regarding particle-based *in-situ* remediation (Georgi et al., 2015). Achieving sufficiently large transport distances before injected particles deposit on the aquifer sediment has been a major issue in developing technologies for particle-based *in-situ* remediation (Macron et al., 2021). Simultaneously, the particles need to be precisely delivered to the target zone and their uncontrolled migration needs to be prevented (Bianco et al., 2017). Particle mobility in saturated porous media such as aquifer sediments is dependent on hydrological and hydrochemical parameters but first of all on particle size (Tufenkii and Elimelech, 2004). Uniform microparticles with a narrow size distribution are thus a prerequisite for controlled placement of a reactive zone in the subsurface without the blockage of sediment pores (Comba and Braun, 2012; Georgi et al., 2015). In addition, for particles with a density close to water, particle diameters in the range of 1 μm yield optimal mobility, facilitating a large radius of influence for each injection of the particle suspension (Tufenkii and Elimelech, 2004).

Consequently, in this work, we aimed at the generation of readily dispersible CS with a narrow size distribution close to 1 μm by HTC of sucrose. For the first time, their colloidal properties were optimized through the addition of CMC as environmentally friendly stabilizer and careful adjustment of the HTC process parameters. Thus, our study helps to address the recently highlighted need for greener and more sustainable products and methods for particle-based *in-situ* remediation (Corsi et al., 2018).

The applicability of CS for contaminant removal was thoroughly characterized using phenanthrene (PHE), a polycyclic aromatic hydrocarbon (PAH) frequently detected in oil-derived groundwater contaminations. The influence of pollutant properties on the sorption affinities of the synthesized material was investigated using a cocktail of different organic

substances with saturated and unsaturated carbon backbones covering a wide range of hydrophobicity and differing in the number and location of chlorine substituents. The chosen pollutants were trichloroethylene (TCE), lindane (LIN), acenaphthene (ACE), hexachlorobenzene (HCB) and 2,3,4-trichlorobiphenyl (TCB). The combined colloid and adsorbent characteristics of the herein synthesized particles show promising application potential in the field of *in-situ* groundwater and soil remediation in case of contamination with hydrophobic compounds.

2. Materials and Methods

2.1. Chemicals

Commercially available sugar was used as starting material for HTC. CMC sodium salt with a molecular weight of about 90 kDa, a polymerization degree of 400, a substitution degree (by $-\text{CH}_2\text{COO}^-$) of 0.65-0.90 with a sodium content of approximately 8 wt.-% and a purity of 99.5 %, was purchased from Sigma-Aldrich. LIN, ACE, PHE (≥ 99.8 %) as well as per-deuterated PHE (98 atom-%) were also purchased from Sigma-Aldrich. Dichloromethane and chloroform (both gas-chromatography grade), potassium hydroxide (p.a.), potassium nitrate (p.a.) and calcium chloride di-hydrate (p.a.) were purchased from Merck. Potassium hydrogen phthalate, TCE, HCB and TCB were all in analytical grade and purchased from Riedel-de Haën.

2.2. Preparation of carbonaceous spheres *via* HTC

For the hydrothermal synthesis of uniform carbonaceous spheres, 0.25-0.75 M sucrose (85.6-256.7 g L⁻¹) dissolved in de-ionized water with 0.3-3 wt.-% of CMC (in relation to initial sucrose) was placed into a stainless steel autoclave with a glass insert. After closing, the autoclave was heated in an oven for 1 to 4 h at 170-200 °C. Comparative experiments were performed in the absence of CMC. The formed precipitate, called hydrochar or CS synonymously, was collected through centrifugation, washed once with de-ionized water and

air-dried. The size distribution and aggregation states of CS were characterized by means of digital microscopy.

2.3. Sedimentation of CS in aqueous media

The dried CS were dispersed in aqueous media at concentrations of 1 and 10 g L⁻¹ using an ultrasonic bath RK 100 SH Sonorex (Bandelin Electronic) with a power of 160 W and a frequency of 35 kHz. The native pH of the samples was measured and an aliquot was taken in order to observe the dispersion of the CS under the digital microscope. The suspensions were then allowed to stand without agitation for 18 h. In order to study the sedimentation of the particles, samples were taken with a syringe from 2 cm below the water surface at 0 h and at 18 h and analyzed using a total organic carbon (TOC) analyzer. The detailed experimental setup is described in the SI part. Furthermore, the sedimentation behavior in the presence of two different salts – KNO₃ and CaCl₂ – in two different pH ranges was investigated exemplarily on the basis of the CS sample synthesized with 0.5 M sucrose, 1 wt.-% CMC (in relation to sucrose) at 180 °C for 2 h (CS_1%). The relative TOC content of the samples taken after 18 h at 2 cm below suspension surface was used as a parameter for comparing the sedimentation behavior of various CS samples.

2.4. Batch sorption experiments

Sorption experiments with PHE were performed in batches with 0.05 g L⁻¹ CS and initial PHE concentrations of 0.01-1.4 mg L⁻¹ at (21 ± 1) °C. Batches with total PHE concentrations close to or above its water solubility were spiked step-wise in portions so that the concentration of PHE in the aqueous phase always remained below the solubility limit. The dried CS were first dispersed in a 1 g L⁻¹ KNO₃ solution by 10 min of ultrasonication, then the appropriate amount of a stock solution of PHE in acetone was added to the mixture. The batches were shaken on a horizontal shaker with 200 rpm for at least 5 days. Kinetic experiments showed that sorption equilibrium was approached before that time, after approximately 48 h, as no significant change

in the aqueous phase concentration of PHE was observed for prolonged contact times. In order to terminate the batch experiments, CS and liquid phase were separated by centrifugation at 4500 rpm for 5 min and the CS as well as the liquid phase were each extracted with chloroform containing 2.5 mg L^{-1} per-deuterated phenanthrene (PHE-D10) as internal standard. The CS were extracted twice with chloroform (mass ratio CS:solvent = 1:1300) in order to close mass balances. The extracts were analyzed by means of gas chromatography with coupled mass-spectrometry (GC-MS). The obtained thermodynamic data for the PHE sorption were fitted according to the Freundlich model using the software OriginPro 2018G (© 1991-2017 OriginLab Corporation). The batch experiment for measuring the single point sorption coefficients of other compounds (TCE, LIN, ACE, HCB and TCB) was conducted analogously in a combined batch with initial concentrations of $10 \text{ } \mu\text{g L}^{-1}$ for each analyte. TCE was analyzed *via* GC-MS of the batch headspace. LIN, ACE, HCB and TCB were extracted analogously to PHE followed by GC-MS analysis of the extracts.

2.5. Analytical methods

Microscopic images were recorded with a VHX digital microscope (Keyence). Random samples of 100-150 particles were measured with the open-source software ImageJ 1.52a in order to determine the particle diameters for the dry CS samples. The measured values were processed with RStudio 1.4 (© 2009-2021 RStudio, PBC) in order to obtain the frequency distribution.

The SEM analyses were conducted with a Zeiss Merlin VP compact. The beam current was 250 pA and the electron landing energy added up to 10 kV.

Elemental (C, H) analysis of the CS samples was conducted with a TruSpec[®] CHN macro-analyzer (LECO). The oxygen content was derived by difference calculation.

The zeta potential was characterized with a Zetasizer Ultra (Malvern Panalytical). Samples were prepared by dispersing the CS in 10 mM KNO₃ at a concentration of 2 mg L⁻¹, and the pH was adjusted to 6 with 1 M KOH.

Temperature-programmed decomposition (TPD) was performed under Ar (50 mL min⁻¹) with a BELCAT-B chemisorption analyzer (BEL). The samples were pretreated at 50 °C for 30 min, heated to 1100 °C with 10 K min⁻¹ and held for 30 min. Evolving CO and CO₂ were detected with an Infracal analyzer (SAXON Junkalor).

The specific surface area (SSA) of the CS was determined with a Belsorp MINI (BEL Japan). Adsorption/desorption of N₂ was performed at -196 °C after pretreatment of the samples under vacuum at 100 °C overnight. The obtained data were evaluated according to the Brunauer-Emmet-Teller (BET) theory.

GC-MS analyses were carried out with a GCMS-QP2010 (Shimadzu). The column (DB-5ms, Agilent) had a length of 30 m, an inner diameter of 0.25 mm and a film thickness of 0.25 µm. For analysis of PHE, 1 µL of the chloroform extract was injected at 250 °C. The following temperature program was used: 60 °C (1 min), with 10 K min⁻¹ to 230 °C and with 30 K min⁻¹ to 290 °C (5 min). The column He flow rate was 1 mL min⁻¹. For the analysis of LIN, ACE, HCB and TCB, the chloroform extracts were injected at 200 °C with an initial column temperature of 100 °C (3 min) and heating with 15 K min⁻¹ to 220 °C (2 min) at a He flow rate of 1.4 mL min⁻¹. TCE was analyzed prior to extraction *via* headspace sampling at an injection temperature of 200 °C and a column temperature of 60 °C with a He flow of 1 mL min⁻¹.

3. Results and Discussion

3.1. Effect of CMC on the morphology of the formed carbonaceous spheres

In order to demonstrate the major effect of the polyelectrolyte CMC during the HTC of sucrose, two different samples were generated: one in the absence (a: CS_0%) and another one in the

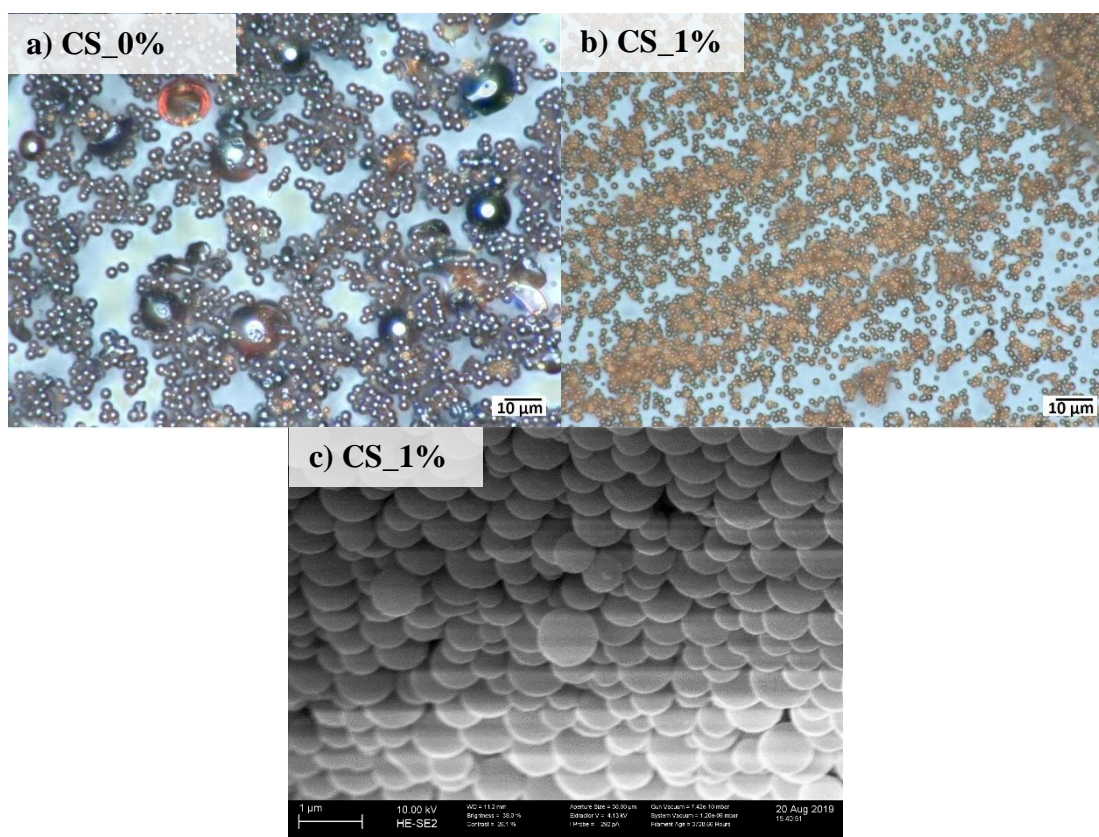


Fig. 1 Digital microscopy (a, b) and SEM analysis (c) of hydrochar prepared from 0.5 M sucrose (a) without and (b,c) with 1 wt.-% CMC (in relation to sucrose) at 180 °C for 2 h.

presence of CMC (b,c: CS_1%). Fig. 1 demonstrates the significant differences between the two CS samples. The particle size distribution of the sample synthesized from sucrose without CMC is broad and reaches from 1 to 10 μm. In contrast, when sucrose was hydrothermally carbonized in the presence of CMC, smaller and uniform CS were formed with a very narrow size range from 0.8 to 1.5 μm (cf. Fig. 1, Tab. 1). Their highly spherical shape was confirmed by SEM analysis (cf. Fig. 1c). The mean particle diameters for samples CS_0% and CS_1% were 1.9 μm and 1.1 μm respectively. As the solid yields of the two samples did not differ significantly (cf. Tab. 1), it can be concluded that the yield of CS in the desired size range of

about 1 μm was significantly increased by addition of CMC. Based on the inter-particle polymerization growth mechanism proposed by Jung *et al.* (2018), one can hypothesize that the CMC adsorbs on freshly formed particles and prevents them from agglomerating and forming larger particles. As CMC is a macromolecular polyelectrolyte with a molecular mass of around 90 kDa, this effect can be ascribed to the enhanced electrostatic repulsion along with sterical hindrance, a so-called electrosteric stabilization effect (Philippe and Schaumann, 2014). Although CMC itself is a carbohydrate, it is obviously sufficiently stable under the applied HTC conditions to provide this stabilizing effect. Thus, it can be used as a cheap and environmentally friendly alternative to previously tested polymers such as e.g. poly(acrylamide) (Tang *et al.*, 2015), which can release toxic acrylamide upon decomposition. In order to synthesize equivalently uniform CS in the absence of CMC, the reaction time had to be reduced to 1 h (see Fig. S5f); however, this was at the expense of a strongly reduced mass yield (only 17 % of the yield after 2 h, Tab 1).

In order to investigate more closely the formation of uniform CS by HTC of sucrose in the presence of CMC, a systematic study was performed whereby the reaction parameters were changed one-by-one and the mean particle diameter as well as the solid yield (defined as the mass of CS divided by the mass of sucrose) was determined and summarized in Tab. 1. The particles were defined as ‘uniform’ when the difference between d_{10} and d_{90} did not exceed 0.6 μm . Please note the extensive material in the supporting information where Figs. S3-S6 provide a visual impression. Uniform CS samples can be distinguished from the irregular ones at first sight under the digital microscope.

Tab. 1: Particle diameter specifications derived from digital microscopy of the dry CS and the according solid yields generated by HTC of sucrose with varying reaction parameters (0-3 wt.-% CMC in relation to sucrose, 0.25-0.75 M sucrose, 1-4 h, 170-200 °C). Limiting upper diameters below which 10, 50 and 90 % of particles could be found (d_{10} , d_{50} , d_{90}) were calculated from random samples of 100-150 particles.

Samples where the difference between d_{90} and d_{10} did not exceed 0.6 μm were considered ‘uniform’ (highlighted in **bold**).

Fixed parameters	Varied parameter	Sample name	Particle size distribution			Yield
			d_{10}	d_{50}	d_{90}	$Y = \frac{m_{\text{CS}}}{m_{\text{sucrose}}}$
			[μm]			[%]
0.5 M sucrose, 180 °C	1 h	CS_0%1h	1.0	1.2	1.5	2.3±0.3
	2 h	CS_0%	1.3	2.2	2.6	13.3±1.0
0.5 M sucrose, 180 °C, 2 h	0.3 % CMC	CS_0.3%	1.3	1.5	3.6	13.0±1.1
	0.5 % CMC	CS_0.5%	1.2	1.4	1.5	13.9±0.7
	1 % CMC	CS_1%	0.9	1.1	1.3	13.7±1.1
	2 % CMC	CS_2%	1.2	1.4	1.6	12.1±0.3
	3 % CMC	CS_3%	1.0	1.4	1.9	14.2±0.2
1 % CMC, 180 °C, 2 h	0.25 M sucrose	CS_0.25M	0.6	0.9	1.1	7.0±0.3
	0.5 M sucrose	CS_0.5M	0.9	1.1	1.3	13.7±1.1
	0.75 M sucrose	CS_0.75M	1.4	1.8	2.6	13.3±0.1
0.5 M sucrose, 1 % CMC, 180 °C	1 h	CS_1h	0.9	1.1	1.2	1.7±0.3
	2 h	CS_2h	0.9	1.1	1.3	13.7±1.1
	3 h	CS_3h	1.1	1.3	1.6	21.0±0.6
	4 h	CS_4h	1.4	1.9	2.4	23.9±1.7
0.5 M sucrose, 1 % CMC, 2 h	170 °C	CS_170C	0.8	0.9	1.1	5.4±0.6
	180 °C	CS_180C	0.9	1.1	1.3	13.7±1.1
	190 °C	CS_190C	1.1	1.4	1.6	20.2±0.2
	200 °C	CS_200C	1.5	1.7	2.0	32.6±0.5

In Tab. 1, it is shown that CMC fractions of 0.5-2 wt.-% related to sucrose proved to be optimal for obtaining uniform CS. CMC concentrations of < 0.5 wt.-% are apparently not sufficient to affect the particle formation mechanism. However, also too high CMC concentrations do not have the desired effect. A similar observation was described by Tang *et al.* (2015) when using poly(acrylamide) as stabilizer – below or above an “ideal” concentration range, the particles

had quite irregular shapes and sizes. This phenomenon was ascribed to the potential crosslinking of spherical particles when too much of the polymer was present (Tang et al., 2015).

Variation of sucrose concentration and reaction time showed that uniform CS could be obtained up to 0.5 M initial sucrose concentration and up to 3 h reaction time. It is worth mentioning that the effect of CMC could still be observed at a reaction temperature as high as 200 °C. This suggests that CMC was stable under these hydrothermal conditions and itself neither hydrolyzed nor carbonized significantly. This is consistent with previous studies where temperatures of 210 °C and higher were required in order to hydrothermally carbonize cellulose (Sevilla and Fuertes, 2009b; Falco et al., 2011; Kang et al., 2012) or CMC (Wu et al., 2016). Furthermore, the hydrolysis of cellulose under hydrothermal conditions occurs only at temperatures ≥ 220 °C, which is indicated by carbonization into microspheres without the retention of the original substrate morphology (Sevilla and Fuertes, 2009b; Dinjus et al., 2011; Falco et al., 2011; Kang et al., 2012; Wu et al., 2016).

It can be assumed that the slow hydrolysis of CMC also becomes relevant at longer reaction times. This could explain why CMC was not effective at a reaction time of 4 h.

The elemental analysis of CS samples resulted in carbon contents of 62.6-65.8 wt.-%, hydrogen contents of 3.9-4.8 wt.-% and derived oxygen contents of 29.9-33.5 wt.-% (cf. Tab. S1). No large differences could be detected for any combination of samples, as the reaction conditions were only varied slightly. Nevertheless, certain expected trends can be seen in Tab. S1 as the C content increases and the O content decreases with increasing sucrose concentration, reaction time and temperature, due to enhanced dehydration of the hydrochars. The observed elemental contents and trends are in good agreement with previous literature studies on the HTC of saccharides (Sevilla and Fuertes, 2009a).

3.2. Dispersibility of the CS and stability in aqueous media

The CS collected after HTC were washed with de-ionized water once and then dried. In order to investigate their actual dispersibility in aqueous media, they were suspended in de-ionized

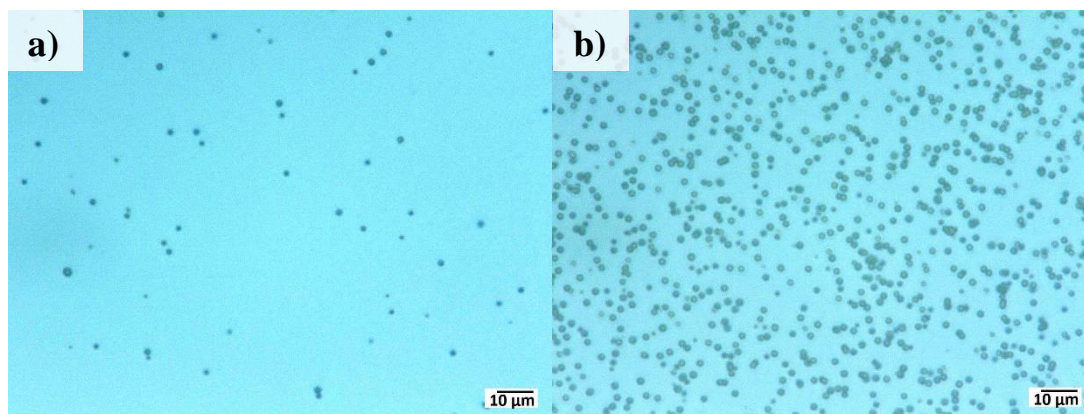


Fig. 2 Digital microscopy images of hydrochar prepared from 0.5 M sucrose and 1 wt.-% CMC (180 °C, 2h) dispersed in de-ionized water with concentrations of a) 1 g L⁻¹ and b) 10 g L⁻¹.

water and subjected to 10 min of ultrasonic treatment (US). Fig. 2 shows the synthesized CS_1%, which are readily dispersed and appear mostly as single spheres when dispersed by US. Even at high concentrations, such as 10 g L⁻¹ (see Fig. 2, b), no larger agglomerates beyond 5 μm were found in the freshly prepared suspensions. An alternative dispersion method is the use of a high-speed homogenizer (e.g. UltraTurrax[®]) which is also applied at technical scale in the field (Mackenzie et al., 2016). For further information see Fig. S14 in the SI. The fact that hydrothermally synthesized CS are well dispersible is due to their high density of functional groups and thus their hydrophilic surface. The dispersibility has been mentioned in a few studies where functional composites were synthesized *via* HTC (Sun and Li, 2004; Wang et al., 2006; Wei et al., 2006; Bai et al., 2010; Zhang et al., 2010), but has rarely been actually investigated (Zhao et al., 2017) and, to the best of our knowledge, never been actually demonstrated. We found that all CS synthesized within this study, which were considered ‘uniform’ based on the particle size distribution as determined by microscopy of the dry sample, could be dispersed into mostly single spheres *via* US (see Fig. S9 – S12) with a low tendency to agglomerate. On the contrary, CS samples which exhibited a broader particle size distribution for the dry sample

were not dispersed into single spheres *via* US (cf. Fig. S9 (a, e), S10 (c), S11 (d)). Therefore, it is deduced that, with proceeding HTC, not only the particle size distribution becomes broader but also the particles become more aggregated. This observation is in line with the proposed growth mechanism by Jung *et al.* (2018) which is based on inter-particle polymerization.

Sample CS_1% showed no significant agglomeration after 1 month storage as non-agitated aqueous suspension, even at a high particle concentration of 10 g L⁻¹ (cf. Fig. S6). This can be explained by means of the Derjaguin-Landau-Verwey-Overbeek (DLVO) theory which states that agglomeration is a function of the frequency of particle collisions and the probability of attachment in the collision events (Sun et al., 2020). As close approach and collisions of the particles cannot be prevented in highly concentrated suspensions, attachment probability needs to be reduced in order to obtain stable suspensions. The synthesized CS_1% particles exhibit a strongly negative zeta potential of -43.5 mV at pH 6 which can be transcribed to a high density of negative surface charges, due to abundant oxygen-containing functional groups (Higgins et al., 2020). The latter were confirmed by TPD analyses, which resulted in a total of 12.3 wt.-% of thermally labile oxygen (data not shown). The determined zeta potential value is higher than the empirical value of $\geq |\pm 30 \text{ mV}|$, which was found as a prerequisite for suspension stability for many types of colloids (Xu, 2000). In such cases, electrostatic repulsion leads to an energy barrier which has to be overcome for agglomeration. Thus, agglomeration phenomena are highly dependent on the ionic strength of the suspension, the ion valence of electrolytes present and the pH of the suspension (Sun et al., 2020).

The suspension stability of the samples produced under various HTC conditions was characterized comparatively by determining the total organic carbon (TOC) content of the resting samples at 0 h (immediately after agitation) and after 18 h at a depth of 2 cm below the suspension surface. This criterion was chosen based on Stokes' law (Eq. (1)), which describes the correlation of particle diameters with sedimentation velocities of spherical particles in suspensions.

$$\frac{d_{\text{Stokes}}}{2} = r = \sqrt{\frac{v_{\text{sedimentation}} \cdot 9\eta}{2(\rho_{\text{particle}} - \rho_{\text{medium}})g}} \quad (1)$$

In Eq. (1), d_{Stokes} is the Stokes diameter of particles (m), $v_{\text{sedimentation}}$ the sedimentation velocity (m s^{-1}), η is the shear viscosity of the medium ($\text{kg m}^{-1} \text{s}^{-1}$), ρ is the density of the particles or the medium respectively (kg m^{-3}), and g is the apparent gravity ($= 9.81 \text{ m s}^{-2}$). The particle density was determined *via* mixing dichloromethane and chloroform in various ratios and observing at which medium density the particles floated in a stable manner for > 60 h. With this method, a mass density of about $(1.45 \pm 0.03) \text{ g cm}^{-3}$ was identified for two representative CS samples synthesized at two different hydrothermal carbonization temperatures: $180 \text{ }^\circ\text{C}$ and $200 \text{ }^\circ\text{C}$. This density was assumed for all synthesized CS samples as the method is not able to determine the suspected minor differences with higher resolution. In the literature, a comparable mass density of 1.445 g cm^{-3} is given for hydrochar pellets prepared from food waste ($220 \text{ }^\circ\text{C}$, 1 h) (Sharma and Dubey, 2020).

According to Stokes' equation (1), particles which pass 2 cm within 18 h are $\geq 1.1 \text{ } \mu\text{m}$ in diameter. Fig. 3 shows that for the CS which were synthesized in the presence of 1 wt.-% CMC,

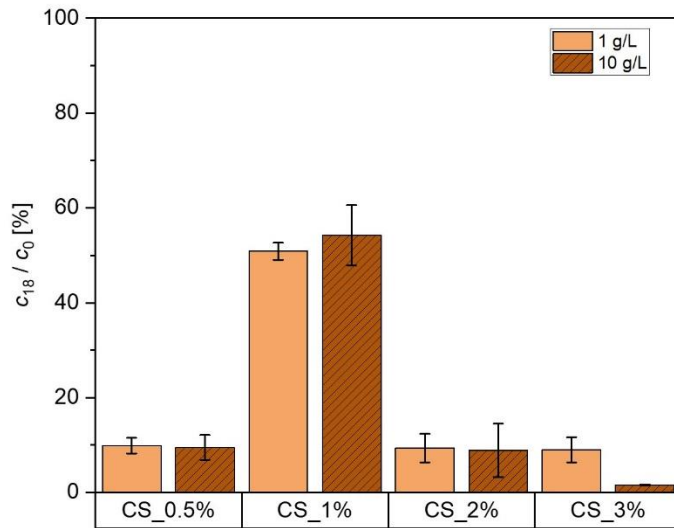


Fig. 3 Suspension stability of various CS samples in de-ionized water (suspended particle fraction after 18 h); the native pH value of the samples was between 3.5 and 4.5; CS were synthesized from 0.5 M sucrose in the presence of various weight percentages of CMC at $180 \text{ }^\circ\text{C}$ for 2 h as detailed in Tab. 1.

a particle mass fraction of 50-60 % did not pass the 2 cm limit, i.e. has a diameter $< 1.1 \text{ } \mu\text{m}$. This is in good accordance with the d_{50} value of $1.2 \text{ } \mu\text{m}$ determined by microscopy (cf. Tab. 1). In contrast, merely $\leq 10 \%$ of the CS samples synthesized in the presence of lower or higher CMC concentrations are still in suspension after 18 h (cf. Fig 3). This can again readily be

explained when referring to Tab. 1, as only 10 % of the particles of these samples have diameters below 1.1 μm .

When comparing the suspension stabilities of all synthesized samples, equivalent trends are visible within the various test series (cf. Fig. S1): the stability of aqueous suspensions decreases with increasing particle diameter. The latter results from a higher initial sucrose concentration, reaction time and/or reaction temperature applied in the HTC process (cf. Fig. 3). Furthermore, the experimental observations of the sedimentation behavior are in good relation with Stokes' law (Eq. (1)). For example, the samples CS_0.25M and CS_170C are the most stable ones where 80-90 % of particles were found in suspension at the 2-cm-sampling point after 18 h. Accordingly, the d_{90} value of these samples can be assumed to be below 1.1 μm , as confirmed by microscopy of the dry particles (Tab. 1). These findings indicate that the sedimentation of particles proceeds practically unhindered and without agglomeration processes. Furthermore, in all cases, higher particle concentrations (causing more frequent collisions) did not lead to faster sedimentation, which in turn speaks against significant agglomeration or, more precisely, for a low probability of attachment in collisions.

In order to investigate how tolerant the suspended CS are to higher ionic strengths, analogous experiments were conducted where 1 g L⁻¹ CS_1% were dispersed in two different electrolyte solutions and again allowed to sediment for 18 h. Various concentrations of KNO₃ and CaCl₂ were applied. It was found that the suspensions “collapsed” at a certain ionic strength, meaning that the particles agglomerated increasingly and completely sedimented within a few hours. As expected, the tolerated salt concentrations depend strongly on the ion valence as well as on the pH of the suspension. At a pH of 4, the particles in suspension of 1 g L⁻¹ CS_1% were present in an agglomerated state at 90 mM KNO₃ (pH 3.8) and 7 mM CaCl₂ (pH 4.1), whereas an analogous suspension tolerated up to 168 mM KNO₃ at pH 6.0 and 12 mM CaCl₂ at pH 6.6 until particles agglomerated (cf. Figs. S8, S9). As a higher ionic strength in the solution leads to the compression of the electric double layer, the particles can approach each other more closely, so

that van-der-Waals interactions predominate and agglomeration occurs (Sun et al., 2020) (Figs. S8, S9). The amount of surface charge, and consequently the thickness of the electric double layer, varies at different pH values. Therefore, the salt concentration which leads to a sufficient compression of the double layer is pH-dependent (Sun et al., 2020), as was also observed within this study.

The tolerated concentration of K^+ was around 13-fold higher (pH 4) and 14-fold higher (pH 6) than that of Ca^{2+} . These results are in accordance with previous findings regarding colloidal particle suspensions. Sun *et al.* (2020) found that colloidal kaolinite suspensions tolerated a 14-fold higher concentration of Na^+ than of Mg^{2+} before the particles agglomerated (Sun et al., 2020). As the ionic strength of a $CaCl_2$ solution is only threefold as high as that of a KNO_3 solution at equal molar concentrations, it can be deduced that specific effects of the bivalent Ca^{2+} lead to a greater destabilization than that due to the effect of monovalent ions. This is also known as the Schulze-Hardy rule. Bivalent ions are, for example, able to form a single ion-layer between two particles and consequently interlink the particles (Trefalt et al., 2020).

3.3. Sorption of various hydrophobic compounds on the hydrothermally synthesized carbonaceous microspheres

The sorption characteristics of the synthesized CS were tested on the basis of the sample CS_1% (0.5 M suc, 1 wt.-% CMC, 180 °C, 2 h) which was chosen due to its desirable colloidal

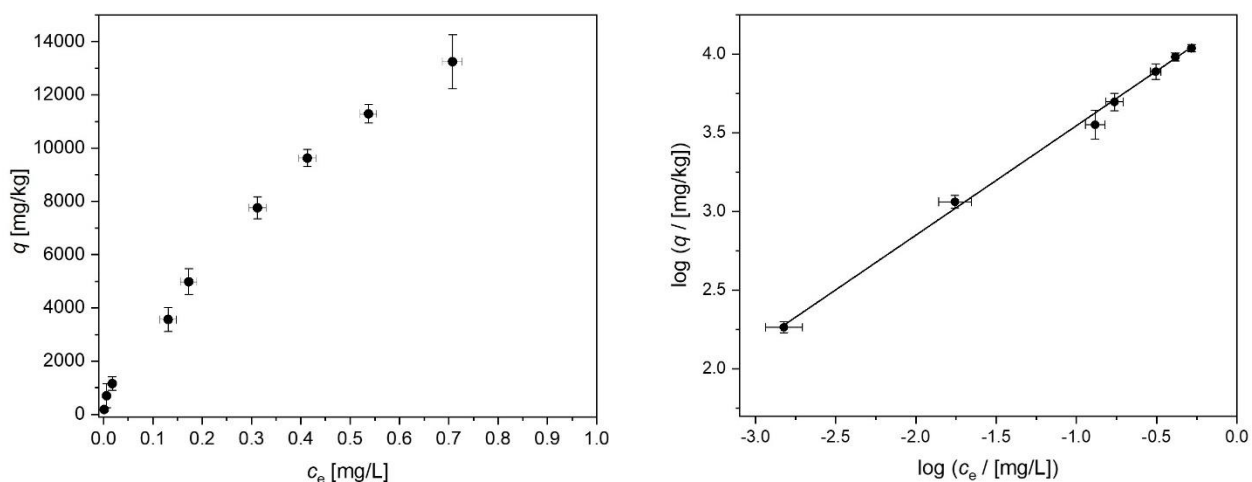


Fig. 4 Sorption of phenanthrene onto hydrothermally synthesized CS (0.5 M suc, 1 wt.-% CMC, 180 °C, 2 h); the last data point of the sorption isotherm showed a relatively high uncertainty (left) and was omitted when fitting according to the linearized Freundlich model (right); error bars were calculated *via* error propagation from the measurement uncertainty regarding the aqueous PHE concentration; $c_{CS} = 50 \text{ mg L}^{-1}$, $c_{0,PHE} = 0.01\text{-}1.4 \text{ mg L}^{-1}$, $c_{KNO_3} = 1 \text{ g L}^{-1}$, pH = 4.8.

properties in combination with a sufficient mass yield. The sorption of PHE was investigated regarding the time frame for approaching an equilibrium state (Fig. S13) and the thermodynamic characteristics (Fig. 4). The sorption isotherm was fitted according to the Freundlich model (eq. 2), where q (mg kg^{-1}) refers to the mass loading, c_e (mg L^{-1}) is the equilibrium concentration of the sorbate in the aqueous phase, K_F is the Freundlich coefficient and n the Freundlich exponent.

$$q = K_F \cdot c_e^{1/n} \quad (2)$$

Fitting the isotherm in Fig. 4 according to eq. 2 leads to $K_F = 17\,500 \text{ (mg kg}^{-1}) \text{ (mg L}^{-1})^{-1/n}$ and $1/n$ of 0.70. As the CS are largely non-porous with a specific surface area $< 5 \text{ m}^2 \text{ g}^{-1}$, the high sorption affinity up to $K_{D,CS} = q/c_e = 10^{5.1} \text{ L kg}^{-1}$ at $c_e = 1.5 \text{ } \mu\text{g L}^{-1}$ and the PHE loading up to 1.3 wt.-% at $c_e = 0.7 \text{ mg L}^{-1}$ lead us to the presumption that an *absorption* process into the

carbonaceous bulk material takes place in addition to the sole *adsorption* onto the particle surface. This was further elucidated by estimating the theoretical maximum loading of the outer particle surface. Based on a calculated smooth geometrical particle surface area of $3.6 \text{ m}^2 \text{ g}^{-1}$ and the approximate monolayer capacity of $1.7 \cdot 10^{-6} \text{ mol m}^{-2}$ PHE (Werner, 2005), the maximum monolayer loading at the outer particle surface would amount to merely 0.1 wt.-%. As the experimentally determined loadings are much higher, it can indeed be assumed that the sorption process of PHE onto the hydrothermally synthesized CS is dominated by absorption into the char. The latter could happen through intercalation of the polyaromatic ring system into the polymer-like carbonaceous material. This so-called partitioning has also been observed for carbonaceous materials such as peat and lignite (Kleineidam et al., 2002). The determined value of the Freundlich exponent $n = 1/0.70 = 1.43$ indicates a heterogeneous composition of the carbonaceous bulk material with more and less sorption affine regions. Similar sorption isotherms have been observed regarding the sorption of polycyclic aromatic hydrocarbons (PAHs) onto organic fractions in soil and sediment (Sun et al., 2010). In additional sorption experiments, we compared the sorption behavior of the CS towards further organic pollutants with different hydrophobicities and with or without presence of aromatic rings and chlorine substituents. In order to eliminate possible competition effects between the different sorbates, the experiments were designed to keep the overall loading below 500 mg kg^{-1} which is only 3 % of the estimated maximum loading of the CS (cf. Fig. 4). Fig. 5 shows a plot of the experimentally determined sorption coefficients ($K_{D,CS}$) of the investigated substances vs. their octanol-water partitioning coefficients (K_{OW}) (Kim et al., 2019). For comparison, we also calculated sorption coefficients to soil organic matter ($K_{D,SOM}$) for the various compounds using the freely accessible UFZ-LSER (linear solvation energy relationship) database (Ulrich et al., 2017) which is based on polyparameter linear free energy relationships (LFER) as common concept for predicting partitioning sorption processes. $K_{D,SOM}$ was calculated by multiplying the distribution coefficient between water and soil organic carbon as obtained from the LSER

database (K_{OC} (Ulrich et al., 2017)) with the mass fraction of organic carbon in peat as model for soil organic matter ($f_{OC} = 0.47$ g C/g peat (Tülp et al., 2009)). In Fig. 5, it can be seen that the sorption affinities of the investigated substances generally increase with increasing K_{OW} as a measure of their hydrophobicity. This is of course expected as substances with higher hydrophobicities tend to leave the water phase and sorb to carbon-rich surroundings. For LIN, ACE and PHE, $K_{D,CS}$ values mirror the K_{OW} values, meaning that the affinities of these substances for octanol and CS are equal. The affinity of the sorbent phase depends on the ability of sorbate and sorbent to take part in various intermolecular interactions. LFER models thus include several parameters such as polarizability and H-bond basicity/acidity of the sorbate and corresponding parameters for the sorbent phase. It is obvious from the differences in $K_{D,CS}$ and $K_{D,SOM}$ that the sorbent properties of both types of carbonaceous materials are not identical and that hydrochar materials such as the studied CS require the development of an individual LSER

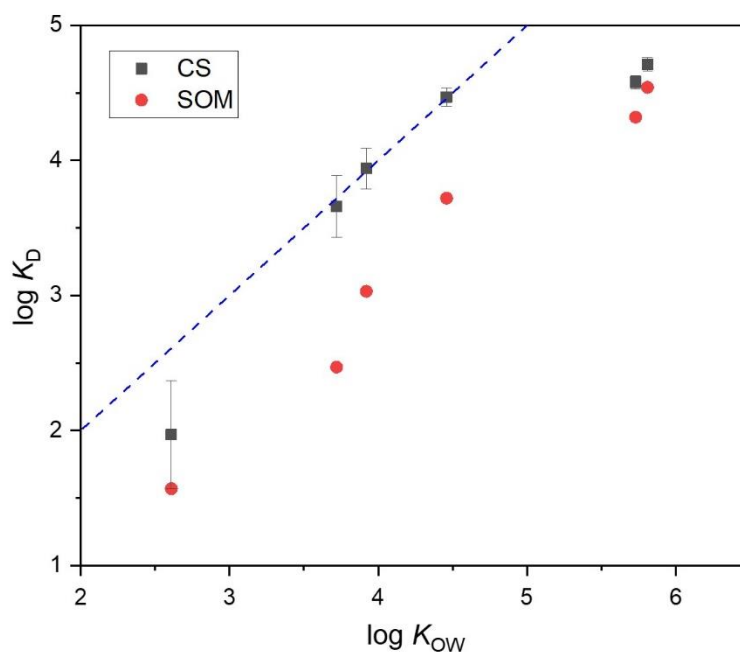


Fig. 5 Experimentally determined sorption coefficient of phenanthrene on CS $\log K_{D,CS}$ ($c_{CS} = 50$ mg L⁻¹, $c_{0,pollutant} = 10$ µg L⁻¹, $c_{KNO_3} = 1$ g L⁻¹, pH = 7.2) in comparison with $\log K_{OW}$ (Kim et al., 2019) and the sorption coefficient on soil organic matter $\log K_{D,SOM}$ based on (Ulrich et al., 2017); the dotted line represents $\log K_{OW} = \log K_D$.

parameter set for the prediction of sorption coefficients. This clearly needs to be based on a large set of experimental sorption data which is a task for future research.

When comparing the $K_{D,CS}$ values for the CS with $K_{D,SOM}$ values, it can be seen that the CS provide higher sorption affinities than peat soil for all probed molecules which is most significant for the compounds with moderate hydrophobicity with factors of 15 (LIN) over 8 (ACE) to 5 (PHE) in $K_{D,CS}$ vs. $K_{D,SOM}$. This means that the synthesized CS could be used at contaminated sites with soils and sediments having low organic matter fractions (such as sandy aquifers) in order to increase the retention capacity and thus prevent the spreading of hydrophobic pollutants with the groundwater flow.

3.4. Estimation of the retardation factor for phenanthrene as well as the effective lifetime of a hypothetical *in-situ* sorption barrier

The effective lifetime of such an *in-situ* sorption barrier was estimated with a model described by Georgi *et al.* (2015). The retardation factor R_{PHE} was calculated with eq. 3 (Georgi *et al.*, 2015) from the experimentally determined single-point sorption coefficient at pH = 7 $K_{D,PHE,CS} = 30\,000\text{ L kg}^{-1}$ at $c_{e,PHE} = 5\text{ }\mu\text{g L}^{-1}$ as the assumed PHE concentration in the contaminated groundwater influent.

$$R_{PHE} = 1 + \frac{\rho}{\varepsilon} f_{CS} K_{D,PHE,CS} \quad (3)$$

ρ (kg L^{-1}) and ε (unitless) are the bulk density and the porosity of the sediment for which typical values of 1.75 kg L^{-1} and 0.3 were supposed (Schwarzenbach *et al.*, 1993). Assuming a fraction $f_{CS} = 0.002$ (= 0.2 wt.-%) of CS immobilized on the sediment, an R_{PHE} of 345 was calculated.

When the latter is put into relation with the average linear velocity of the groundwater u (m d^{-1}) and a length of the sorption barrier l (m) in the direction of the groundwater flow, the useable lifetime t (d) of the sorption barrier can be calculated according to eq. 4 (Georgi *et al.*, 2015):

$$t = \frac{l}{u} \cdot R_{PHE} \quad (4)$$

This is a simplified approach which assumes a step-function breakthrough curve, i.e. approaching sorption equilibria during the slow passage of groundwater through the sorption barrier, and neglecting dispersion effects. Nevertheless, it provides a first estimate on expected useable operation times of *in-situ* sorption barriers. With an assumed groundwater velocity of 0.5 m d^{-1} and a barrier length of 10 m (Georgi et al., 2015), the estimated lifetime of the *in-situ* sorption barrier with the herein synthesized CS would be 19 years regarding the retention of PHE as a typical 3-ring PAH representative of oil-derived hydrophobic pollutants detected in groundwater. More hydrophobic compounds such as PAHs with 4 and more rings or the tested HCB and TCB can be reasonably predicted to have even longer breakthrough times (see SI, Tab. S2). For LIN and ACE ($\log K_{\text{OW}} > 3$), the predicted retention times in the order of 3-6 years are still noteworthy while the remediation approach is not suitable for less hydrophobic contaminants such as TCE ($\log K_{\text{OW}} < 3$).

The measured sorption kinetics (see SI, Fig. S13) yields a half-life of about 15 h for approaching sorption equilibrium with PHE under batch conditions in a shaken suspension. This indicates a relatively slow sorption process compared to activated carbon particles of comparable size (Grathwohl, 1998). The finding is in conformity with the dominating sorption mechanism and the assumed rate-controlling process: bulk phase diffusion in a highly viscous polymer-like phase of the CS particles, in contrast to activated carbon particles where the film or pore diffusion in an aqueous medium are the slowest steps of the adsorption process. Nevertheless, the sorption process is still sufficiently fast to approach sorption equilibria under *in-situ* conditions, taking into account the long residence times ($\tau = \text{barrier length} / \text{groundwater velocity}$) of groundwater in a permeable sorption barrier. An assumed groundwater velocity of 0.5 m d^{-1} and a barrier length of 10 m (Georgi et al., 2015) lead to a residence time of 20 d, which would be completely sufficient to approach sorption equilibrium (cf. Fig S13).

4. Conclusion

Uniform and dispersible CS with tunable mean particle diameters from 1-1.5 μm were synthesized within a single step *via* HTC of sucrose in the presence of CMC as a cheap, non-toxic and environmentally friendly polyelectrolyte stabilizer. The synthesized uniform CS samples were dispersible into single spheres in water, and suspensions remained stable over several hours. Due to these excellent colloidal properties, CS are suitable for *in-situ* application in aquifers using simple infiltration processes. High sorption coefficients of up to $K_{D,CS} = 10^5 \text{ L kg}^{-1}$ were found for phenanthrene (at low concentrations of about $10 \mu\text{g L}^{-1}$) combined with high sorption capacities of CS, $> 1 \text{ wt.-%}$. This indicates absorption as the dominating sorption mechanism for hydrophobic pollutants. The obtained results are promising for the potential application of the hydrothermally synthesized CS in *in-situ* sorption barriers providing an alternative to finely-ground activated carbon colloids at least for hydrophobic pollutants such as PAHs, with predicted operating lifetimes in the range of several decades. Benefits of the proposed synthesis method are the renewable carbon source, the bottom-up generation of highly uniform microparticles in the desired size range and the anticipated smaller “carbon footprint” due to the absence of a high-temperature ($T \geq 600 \text{ }^\circ\text{C}$) activation/pyrolysis procedure such as typically applied in activated carbon production. This encourages further studies in terms of up-scaling of the process, also including the search for suitable waste carbon sources, e.g. from food-grade sugar production. Preliminary experiments suggest that – due to the CMC as stabilizing agent – the herein described process is also applicable to more complex feedstocks with a greater amount of impurities like sugar beet syrup. Further studies should also involve experiments on the mobility of the synthesized CS particles in real aquifer matrices which is an essential requirement for installing *in-situ* sorption barriers. The highly uniform spherical shape and size around $1 \mu\text{m}$ in combination with the strongly negative zeta potential (-43.5 mV at

pH = 6) of the particles provide excellent conditions for high subsurface mobility with low tendency of blocking the passages.

Acknowledgement

The authors acknowledge the financial support from “Deutsche Forschungsgemeinschaft” (DFG), project number 392011053.

They also thank Dr. Matthias Schmidt for the SEM analysis which was done at ProVIS – Centre for Chemical Microscopy at the UFZ, Leipzig, which is supported by European Regional Development Funds (EFRE-Europe funds Saxony) and the Helmholtz Association.

Furthermore, the authors sincerely thank Birgit Würz for kindly assisting with the zeta potential measurement which was performed at the Department of Environmental Microbiology of the UFZ, Leipzig.

Last but not least, the authors are much obliged to Birgit Forkert, Kerstin Lehmann, Dr. Robert Köhler and Silke Woszidlo from the Department of Environmental Engineering (UFZ, Leipzig) for their support by conducting the BET analysis, the elemental analysis of the synthesized particles and additional sorption experiments.

Appendix A. Supplementary data

Supplementary data to this article can be found online.

Literature

- Bai, L., Mei, B., Guo, Q.-Z., Shi, Z.-G., Feng, Y.-Q., 2010. Magnetic solid-phase extraction of hydrophobic analytes in environmental samples by a surface hydrophilic carbon-ferromagnetic nanocomposite. *Journal of Chromatography A* 1217, 7331-7336.
- Bardos, P., Merly, C., Kvapil, P., Koschitzky, H.-P., 2018. Status of nanoremediation and its potential for future deployment: Risk-benefit and benchmarking appraisals. *Remediation Journal* 28, 43-56.
- Bianco, C., Higuera, J.E.P., Tosco, T., Tiraferri, A., Sethi, R., 2017. Controlled deposition of particles in porous media for effective aquifer nanoremediation. *Sci. Rep.* 7, 12992.
- Cai, H., Lin, X., Tian, L., Luo, X., 2016. One-step hydrothermal synthesis of carbonaceous spheres from glucose with an aluminum chloride catalyst and its adsorption characteristic for uranium(VI). *Industrial & Engineering Chemistry Research* 55, 9648-9656.
- Carey, G.R., McGregor, R., Pham, A.L., Sleep, B., Hakimabadi, S., 2019. Evaluating the longevity of a PFAS in situ colloidal activated carbon remedy. *Remediation J.*, 17-31.
- Chowdhury, Z.Z., Krishnan, B., Sagadevan, S., Rafique, R.F., Hamizi, N.A.B., Wahab, Y.A., Khan, A.A., Johan, R.B., Al-douri, Y., Kazi, S.N., Shah, S.T., 2018. Effect of temperature on the physical,

electro-chemical and adsorption properties of carbon micro-spheres using hydrothermal carbonization process. *Nanomaterials* 8, 597-616.

Comba, S., Braun, J., 2012. A new physical model based on cascading column experiments to reproduce the radial flow and transport of micro-iron particles. *Journal of Contaminant Hydrology* 140-141, 1-11.

Corsi, I., Winther-Nielsen, M., Sethi, R., Punta, R., Torre, D.C., Libralato, G., Lofrano, G., Sabatini, L., Aiello, M., Fiordi, L., Cinuzzi, F., Caneschi, A., Pellegrini, D., Buttino, I., 2018. Ecofriendly nanotechnologies and nanomaterials for environmental applications: Key issue and consensus recommendations for sustainable and ecosafe nanoremediation. *Ecotoxicol. Environ. Saf.* 154, 237-244.

Dinjus, E., Kruse, A., Tröger, N., 2011. Hydrothermale Karbonisierung: 1. Einfluss des Lignins in Lignocellulosen. *CIT* 83, 1734.

Falco, C., Baccile, N., Titirici, M.M., 2011. Morphological and structural differences between glucose, cellulose and lignocellulosic biomass derived hydrothermal carbons. *Green Chemistry* 13, 3273-3281.

Georgi, A., Schierz, A., Mackenzie, K., Kopinke, F.-D., 2015. Colloidal activated carbon for in-situ groundwater remediation - Transport characteristics and adsorption of organic compounds in water-saturated sediment columns. *Journal of Contaminant Hydrology* 179, 76-88.

Gong, Y., Xie, L., Li, H., Wang, Y., 2014. Sustainable and scalable production of monodisperse and highly uniform colloidal carbonaceous spheres using sodium polyacrylate as the dispersant. *Chemical Communications* 50, 12633-12636.

Grathwohl, P., 1998. Diffusion in natural porous media: Contaminant transport, sorption/desorption and dissolution kinetics. Springer, Berlin.

Higgins, L.J.R., Brown, A.P., Harrington, J.P., Ross, A.B., Kaulich, B., Mishra, B., 2020. Evidence for a core-shell structure of hydrothermal carbon. *Carbon* 161, 423-431.

Hu, B., Wang, K., Wu, L., Yu, S.-H., Antonietti, M., Titirici, M.-M., 2010. Engineering carbon materials from the hydrothermal carbonization process of biomass. *Adv. Mater.* 22, 813-828.

Intrapore, 2022. Particle-based ground-water remediation. <https://intrapore.com/en/>, accessed on 21.05.2022.

Jain, A., Balasubramanian, R., Srinivasan, M.P., 2016. Hydrothermal conversion of biomass waste to activated carbon with high porosity: A review. *Chem. Eng. J.* 283, 789-805.

Jung, D., Zimmermann, M., Kruse, A., 2018. Hydrothermal carbonization of fructose: Growth mechanism and kinetic model. *ACS Sustainable Chemistry & Engineering* 6, 13877-13887.

Kang, S., Li, X., Fan, J., Chang, J., 2012. Characterization of hydrochars produced by hydrothermal carbonization of lignin, cellulose, D-xylose, and wood meal. *Industrial & Engineering Chemistry Research* 51, 9023-9031.

Kim, S., Chen, J., Cheng, T., Gindulyte, A., He, J., He, S., Li, Q., Shoemaker, B.A., Thiessen, P.A., Yu, B., Zaslavsky, L., Zhang, J., Bolton, E.E., 2019. PubChem in 2021: new data content and improved web interfaces. *Nucleic Acids Res.* 49, D1388-D1395.

Kleineidam, S., Schüth, C., Grathwohl, P., 2002. Solubility-normalized combined adsorption-partitioning sorption isotherms for organic pollutants. *Environ. Sci. Technol.* 36, 4680-4697.

Kubo, S., White, J.R., Tauer, K., Titirici, M.M., 2013. Flexible coral-like carbon nanoarchitectures via a dual block copolymer-latex templating approach. *Chemistry of Materials* 25, 4781-4790.

LaMer, V.K., 1952. Nucleation in phase transitions. *Ind. Eng. Chem.* 44, 1270-1277.

Li, R., Shahbazi, A., 2015. A review of hydrothermal carbonization of carbohydrates for carbon spheres preparation. *Trends in Renewable Energy* 1, 43-56.

Li, S., Liang, F., Wang, J., Zhang, H., Zhang, S., 2017. Preparation of mono-dispersed carbonaceous spheres via a hydrothermal process. *Advanced Powder Technology* 28, 2648-2657.

Liang, M., Wang, J., Zhao, M., Cai, J., Zhang, M., Deng, N., Wang, B., Li, B., Zhang, K., 2019. Borax-assisted hydrothermal carbonization to fabricate monodisperse carbon spheres with high thermostability. *Materials Research Express* 6.

Liu, C., He, Y., Wei, L., Zhang, Y., Zhao, Y., Hong, J., Chen, S., Wang, L., Li, J., 2018a. Hydrothermal carbon-coated TiO₂ as support for co-based catalyst in Fischer-Tropsch synthesis. *ACS Catalysis* 8, 1591-1600.

Liu, P., Cai, W., Wei, J., Cai, Z., Zhu, M., Han, B., Yang, Z., Chen, J., Jaroniec, M., 2019. Ultrafast preparation of saccharide-derived carbon microspheres with excellent dispersibility via ammonium persulfate-assisted hydrothermal carbonization. *J. Mater. Chem. A* 7, 18840-18845.

Liu, Y., Ma, S., Chen, J., 2018b. A novel pyro-hydrochar via sequential carbonization of biomass waste: preparation, characterization and adsorption capacity. *Journal of Cleaner Production* 176, 187-195.

Mackenzie, K., Bleyl, S., Kopinke, F.-D., Doose, H., Bruns, J., 2016. Carbo-Iron as improvement of the nanoiron technology: From laboratory design to the field test. *Sci. Total Environm.* 563-564, 641-648.

Mackenzie, K., Georgi, A., 2019. NZVI synthesis and characterization. in: Phenrat, T., Lowry, G.V. (Eds.). *Nanoscale zerovalent iron particles for environmental restoration*. Springer International Publishing AG, Basel, pp. 45-95.

Mackenzie, K., Schierz, A., Georgi, A., Kopinke, F.-D., 2008. Colloidal activated carbon and CARBO-IRON - Novel materials for in-situ groundwater treatment. *Glob. NEST J.* 10, 54-61.

Macron, L., Oliveras, J., Puentes, V.F., 2021. *In situ* nanoremediation of soils and groundwaters from the nanoparticle's standpoint: A review. *Sci. Total Environm.* 791, 148324.

Nizamuddin, S., Baloch, H.A., Griffin, G.J., Mubarak, N.M., Bhutto, A.W., Abro, R., Mazari, S.A., Ali, B.S., 2017. An overview of effect of process parameters on hydrothermal carbonization of biomass. *Renew. Sust. Energ. Rev.* 73, 1289-1299.

Philippe, A., Schaumann, G.E., 2014. Interactions of dissolved organic matter with natural and engineered inorganic colloids - a review. *Environ. Sci. Technol.* 48, 8946-8962.

Regenesis, 2022. PlumeStop® Liquid Activated Carbon™. <https://regenesis.com/en/remediation-products/plumestop-liquid-activated-carbon/>, accessed on 21.05.2022.

Schwarzenbach, R.P., Gschwend, P.M., Imboden, D.M., 1993. *Environmental Organic Chemistry*. John Wiley and Sons Inc., New York.

Sevilla, M., Fuertes, A.B., 2009a. Chemical and structural properties of carbonaceous products obtained by hydrothermal carbonization of saccharides. *Chem. Eur. J.* 15, 4195-4203.

Sevilla, M., Fuertes, A.B., 2009b. The production of carbon materials by hydrothermal carbonization of cellulose. *Carbon* 47, 2281-2289.

Sharma, H.B., Dubey, B.K., 2020. Co-hydrothermal carbonization of food waste with yard waste for solid biofuel production: Hydrochar characterization and its pelletization. *Waste Management* 118, 521-533.

Sorengard, M., Berggren Kleja, D., Ahrens, L., 2019. Stabilization of per- and polyfluoroalkyl substances (PFASs) with colloidal activated carbon (PlumeStop (R)) as a function of soil clay and organic matter content. *J. Environ. Manage.* 249.

Su, J., Fang, C., Yang, M., Cheng, Y., Wang, Z., Huang, Z., You, C., 2020. A controllable soft-templating approach to synthesize mesoporous carbon microspheres derived from D-xylose via hydrothermal method. *Journals of Materials Science & Technology* 38, 183-188.

Sun, K., Gao, B., Zhang, Z., Zhang, G., Zhao, Y., Xing, B., 2010. Sorption of atrazine and phenanthrene by organic matter fractions in soil and sediment. *Environ. Pollut.* 158, 3520-3526.

Sun, X., Li, Y., 2004. Colloidal carbon spheres and their core/shell structures with noble-metal nanoparticles. *Angew. Chem.* 116, 607-611.

Sun, Y., Pan, D., Wei, X., Xian, D., Wang, P., Hou, J., Xu, Z., Liu, C., Wu, W., 2020. Insight into the stability and correlated transport of kaolinite colloid: Effect of pH, electrolytes and humic substances. *Environ. Pollut.* 266, Article 115189.

Tang, C., Pingping, Z., Sun, Y., Bai, L., 2015. Size-tunable synthesis of mono-disperse wastewater-derived carbon spheres with polyacrylamide as a directing agent. *Micro Nano Lett.* 10, 603-606.

Titirici, M.-M., Thomas, A., Antonietti, M., 2007. Replication and coating of silica templates by hydrothermal carbonization. *Adv. Funct. Mater.* 17, 1010-1018.

Titirici, M.M., Antonietti, M., 2010. Chemistry and materials options of sustainable carbon materials made by hydrothermal carbonization. *Chemical Society Reviews* 39, 103-116.

Trefalt, G., Szilágyi, I., Borkovec, M., 2020. Schulze-Hardy rule revisited. *Colloid Polym. Sci.* 298, 961-967.

Tufenkii, N., Elimelech, M., 2004. Correlation equation for predicting single-collector efficiency in physicochemical filtration in saturated porous media. *Environ. Sci. Technol.* 38, 529-536.

Tülp, H.C., Fenner, K., Schwarzenbach, R.P., Goss, K.-U., 2009. pH-Dependent Sorption of Acidic Organic Chemicals to Soil Organic Matter. *Environ. Sci. Technol.* 43, 9189-9195.

Ulrich, N., Endo, S., Brown, T.N., Watanabe, N., Bronner, G., Abraham, M.H., Goss, K.-U., 2017. UFZ-LSER database v 3.2.1, Leipzig, Germany, Helmholtz-Centre for Environmental Research-UFZ.

Wang, Z., Guo, H., Yu, Y., He, N., 2006. Synthesis and characterization of a novel magnetic carrier with its composition of Fe₃O₄/carbon using hydrothermal reaction. *Journal of Magnetism and Magnetic Materials* 302, 397-404.

Wei, X.-W., Zhu, G.-X., Xia, C.-J., Ye, Y., 2006. A solution phase fabrication of magnetic nanoparticles encapsulated in carbon. *Nanotechnology* 17, 4307-4311.

Werner, D., 2005. Comment on "Modelling maximum adsorption capacities of soot and soot-like materials for PAHs and PCBs". *Environ. Sci. Technol.* 39, 381-382.

White, J.R., Tauer, K., Antonietti, M., Titirici, M.M., 2010. Functional hollow carbon nanospheres by latex templating. *JACS Communications* 132, 17360-17363.

Wu, Q., Li, W., Liu, S., Jin, C., 2016. Hydrothermal synthesis of N-doped spherical carbon from carboxymethylcellulose for CO₂ capture. *Applied Surface Science* 369, 101-107.

Xu, R., 2000. Particle characterization: light scattering methods. Springer, Netherlands.

Yang, H., Wang, G., Ding, N., Yin, C., Chen, Y., 2016. Size-controllable synthesis of carbon spheres with assistance of metal ions. *Synthetic Metals* 214, 1-4.

Yang, J., Li, J.-Y., Qian, J.-Q., Lian, H.-Z., Chen, H.-Y., 2014. Solid phase extraction of magnetic carbon doped Fe₃O₄ nanoparticles. *Journal of Chromatography A* 1325, 8-15.

Yang, Z.-C., Zhang, Y., Kong, J.-H., Wong, S.-Y., Li, X., Wang, J., 2013. Hollow carbon nanoparticles of tunable size and wall thickness by hydrothermal treatment of α -Cyclodextrin templated by F127 block copolymers. *Chemistry of Materials* 25, 704-710.

Zhang, S., Niu, H., Hu, Z., Cai, Y., Shi, Y., 2010. Preparation of carbon coated Fe₃O₄ nanoparticles and their application for solid-phase extraction of polycyclic aromatic hydrocarbons from environmental water samples. *Journal of Chromatography A* 1217, 4757-4764.

Zhang, T., Lowry, G.V., Capiro, N.L., Chen, J., Chen, W., Chen, Y., Dionysiou, D.D., Elliott, D.W., Ghoshal, S., Hofmann, T., Hsu-Kim, H., Liu, S., Ma, J., Pan, B., Phenrat, T., Qu, X., Quan, X., Saleh, V., Vikesland, P.J., Wang, Q., Westerhoff, P., Wong, M.S., Xia, T., Xing, B., Yan, B., Zhang, L., Zhou, D., Alvarez, P.J.J., 2019. *In situ* remediation of subsurface contamination: opportunities and challenges for nanotechnology and advanced materials. *Environ. Sci.: Nano* 6, 1283-1302.

Zhao, Q., Wu, S., Zhang, P., Zhu, Y., 2017. Green polyelectrolyte-functionalization of carbonaceous nanospheres and its application in ion chromatography. *ACS Sustainable Chemistry & Engineering* 5, 112-118.

Zhao, X., Li, W., Liu, S.-X., 2013. Coupled soft-template/hydrothermal process synthesis of mesoporous carbon spheres from liquefied larch sawdust. *Materials Letters* 107, 5-8.

Zheng, M., Liu, Y., Xiao, Y., Zhu, Y., Guan, Q., Yuan, D., Zhang, J., 2009. An easy catalyst-free hydrothermal method to prepare monodisperse carbon microspheres on a large scale. *J. Phys. Chem. C* 113, 8455-8459.